Title

Uranyl/12-crown-4 Ether Complexes and Derivatives: Structural Characterization and Isomeric Differentiation

Journal

Inorganic Chemistry, 57(7)

ISSN

0020-1669

Authors

Jian, Jiwen
Hu, Shu-Xian
Li, Wan-Lu
et al.

Publication Date

2018-04-02

DOI

10.1021/acs.inorgchem.8b00306

Uranyl-(12-Crown-4) Ether Complexes and Derivatives: Structural Characterization and Isomeric Differentiation

Jiwen Jian, [a,†] Shu-Xian Hu,[b,c,†] Wan-Lu Li,[c] Michael J. van Stipdonk,[d] Jonathan Martens,[e]

Giel Berden,[e] Jos Oomens,[e,f] Jun Li [c,*], John K. Gibson[a,*]

[a]*Chemical Sciences Division, Lawrence Berkeley National Laboratory, Berkeley, California 94720, USA*

[b] *Beijing Computational Science Research Center, Beijing 100193, China*

[c] *Department of Chemistry and Key Laboratory of Organic Optoelectronics & Molecular Engineering of Ministry of Education, Tsinghua University, Beijing 100084, China*

[d]*Department of Chemistry and Biochemistry, Duquesne University, Pittsburgh, Pennsylvania 15282 USA*

[e]*Radboud University, Institute for Molecules and Materials, FELIX Laboratory, Toernooiveld 7c, 6525ED Nijmegen, The Netherlands*

[f]*van't Hoff Institute for Molecular Sciences, University of Amsterdam, Science Park 904, 1098XH Amsterdam, The Netherlands*

[†]These authors contributed equally to this work.

[*]Corresponding authors email addresses: junli@tsinghua.edu.cn (Li); jkgibson@lbl.gov (Gibson)

Abstract

The following gas-phase uranyl/12-Crown-4 (12C4) complexes were synthesized by electrospray ionization: $[UO_2(12C4)_2]^{2+}$ and $[UO_2(12C4)_2(OH)]^+$. Collision induced dissociation (CID) of the dication resulted in $[UO_2(12C4\text{-}H)]^+$ (12C4-H is a 12C4 that has lost one H), which spontaneously adds water to yield $[UO_2(12C4\text{-}H)(H_2O)]^+$. The latter has the same composition as $[UO_2(12C4)(OH)]^+$ produced by CID of $[UO_2(12C4)_2(OH)]^+$ but exhibits different reactivity with water. The postulated structures as isomeric $[UO_2(12C4\text{-}H)(H_2O)]^+$ and $[UO_2(12C4)(OH)]^+$ were confirmed by comparison of infrared multiphoton dissociation (IRMPD) spectra with computed spectra. The structure of $[UO_2(12C4\text{-}H)]^+$ corresponds to cleavage of a C-O bond in the 12C4 ring, with formation of a discrete U-O_{eq} bond and equatorial coordination by three intact ether moieties. Comparison of IRMPD and computed IR spectra furthermore enabled assignment of the structures of the other complexes. Theoretical studies of the chemical bonding features of the complexes provide understanding of their stabilities and reactivities. The results reveal bonding and structures of the uranyl/12C4 complexes, and demonstrate the synthesis and identification of two different isomers of gas-phase uranyl coordination complexes.

Introduction

The coordination chemistry of actinide ions with polydentate macrocyclic ligands is of particular interest in the context of actinide partitioning from nuclear waste.[1-3] Crown ethers[4] are known to form complexes with specific metal cations due to the match between cavity size and metal radii,[4,5] which makes these ligands appealing because of the possibility of providing a specific fit for an ion by modifying the size of the crown cavity. Two common crown ether binding motifs are inclusion and outer-sphere complexes, depending on whether the metal center is encapsulated by the crown ether or partly exposed (Scheme 1).[4,6]

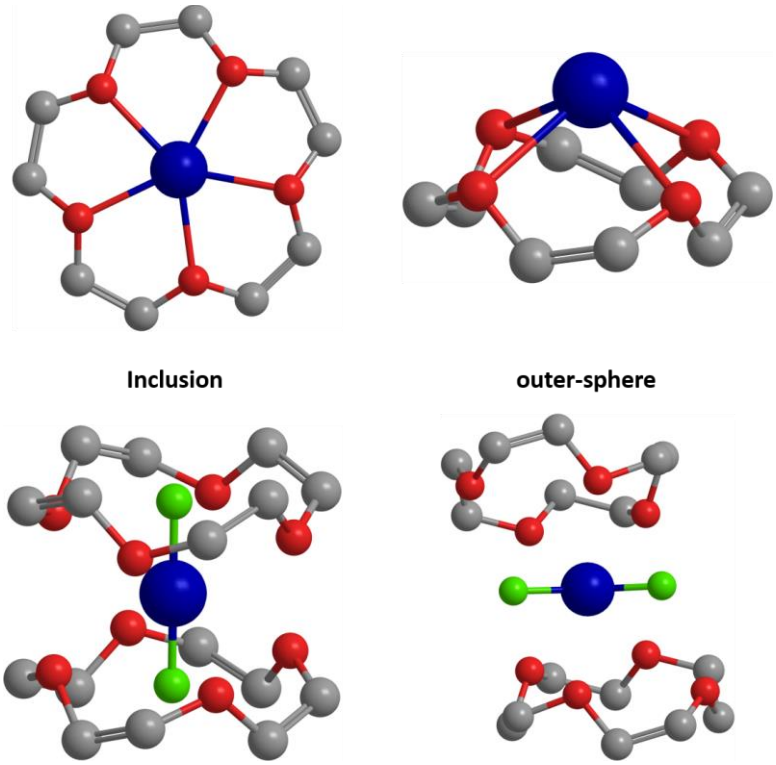

Scheme 1. Inclusion (left) and outer-sphere (right) structures of metal- (upper) and uranyl- (bottom) crown ether (15C5 and 12C4) complexes (H atoms are not shown). For clarity the crown ether atoms are red and the uranyl O atoms are green.

Most of solid state actinide-crown ether studies involve uranyl(VI) complexes. Crystallization from aqueous solutions results in the formation of a fully hydrated UO_2^{2+} core with second-shell crown ethers interacting with inner-shell H_2O molecules via hydrogen bonding.[7-10] Inclusion complexes in which UO_2^{2+} is encapsulated by the crown ether are only

achieved under anhydrous conditions.[11,12] In solution, inclusion of a metal ion into the crown ring depends strongly on the solvent used.[13] Only one crown ether complex has been structurally characterized for transuranium elements in solution: NpO_2^+ was encapsulated in 18-Crown-6 (18C6) by reaction of NpO_2^{2+}/NpO_2^+ with 18C6 in aqueous solution.[14] Relativistic density functional theory (DFT) studies on the $[AnO_2(18C6)]^q$ (q = +1, +2; An = U, Np, Pu) complexes[15] have suggested that the preference for the formation of pentavalent $[NpO_2(18C6)]^+$ rather than hexavalent $[NpO_2(18C6)]^{2+}$ in aqueous solution is consequence of a combined effect of solvation in polar solvents and the effective screening of charge provided by the crown ether.

In a recent report, a series of 12-Crown-4 (12C4), 15-Crown-5 (15C5) and 18C6 complexes of uranyl, neptunyl and plutonyl with a metal-to-ligand ratio of 1:1 were synthetized in the gas phase;[16] 1:2 complexes were also prepared in the case of 15C5 and 12C4. From hydration properties it was concluded that 1:1 actinyl-crown ether complexes exhibit either inclusion or outer-coordination (*side-on*) structures depending on the cavity size. 18C6 provides the best fit for actinyls, forming inclusion complexes with all the pentavalent actinyls, AnO_2^+ (An= U, Np, Pu), as well as with hexavalent uranyl. 12C4 is too small to encapsulate actinyls, whereas 15C5 lies between 12C4 and 18C6 in accommodating actinyl inclusion, as reflected by the formation of both inclusion and outer-coordination isomers depending on the preparative conditions. In the case of 18C6 and hexavalent uranyl, only 1:1 inclusion complexes were synthesized, while 15C5 and 14C4 formed outer-coordination 1:1 complexes, which were able to add a second ligand to yield 1:2 *sandwich* complexes. More recently, the gas-phase $[UO_2(15C5)_2]^{2+}$ complex was characterized by infrared spectroscopy and quantum chemical studies.[17] It was determined that the lowest-energy isomer comprises an outer-sphere *sandwich* structure with an unusual non-perpendicular orientation.[17]

Using the same approach, we here analyze the structural and bonding properties of the two cations initially formed by electrospray ionization, $[UO_2(12C4)_2]^{2+}$ and $[UO_2(12C4)_2(OH)]^+$, as well as derivative ions prepared by collision induced dissociation (CID) of $[UO_2(12C4)_2(OH)]^+$ to yield $[UO_2(12C4)(OH)]^+$, CID of $[UO_2(12C4)_2]^{2+}$ to yield $[UO_2(12C4\text{-}H)]^+$, and water addition to the latter to produce $[UO_2(12C4\text{-}H)(H_2O)]^+$. Theoretical studies are performed to obtain the geometric parameters and bonding properties of these complexes.

Experimental Methods

The formation of uranyl-12C4 complexes by ESI, and their CID and water-addition chemistry, was studied at LBNL using an Agilent 6340 quadrupole ion trap mass spectrometer (QIT/MS). The approach has been described elsewhere, including for studies of hydration of uranyl-crown complexes.[16] The $[UO_2(12C4)_2]^{2+}$ and $[UO_2(12C4)_2OH]^{+}$ complexes were produced by ESI of a solution of ~100 µM uranyl chloride and ~400 µM 12C4 (Sigma-Aldrich ≥98%) in ethanol (<10% water). The background water pressure in the ion trap is sufficiently high (~10^{-6} Torr) for spontaneous hydration of complexes when energetically and kinetically favorable.[18] CID was performed by isolating and resonantly exciting ions with a specific mass-to-charge ratio (m/z), which results in multiple collisions with the He bath gas (~10^{-4} Torr) and in fragmentation when an adequate excitation voltage is applied. Spontaneous reactions with background water in the ion trap were studied by isolating a specific m/z and applying a fixed time delay during which ion-molecule reactions can occur. When hydration is sufficiently facile, it is observed during the ~50 ms CID timescale without application of an additional reaction time.

The intensity distributions of ions in the mass spectra are highly dependent on instrumental parameters, particularly the RF voltage (trap drive) applied to the ion trap; the optimized parameters used for trapping singly- and doubly-charged cations are similar to those employed in previous experiments.[19] In general, a higher trap drive favors trapping cations with higher m/z (z = 1), while efficient trapping of cations with lower m/z (z = 2) requires a lower trap drive. In particular, it has been demonstrated that trapping conditions induced by a lower-voltage trap drive favors retention in the ion trap of doubly-charged actinyl cations.[20]

The infrared multiple photon dissociation (IRMPD) experiments were performed at the Free Electron Laser for Infrared eXperiments (FELIX) Laboratory[21]. The $[UO_2(12C4)_2]^{2+}$ and $[UO_2(12C4)_2OH]^{+}$ complexes were produced by ESI of a solution of ~10 µM uranyl perchlorate and ~40 µM 12C4 in ethanol (<10% water). The IRMPD spectra were acquired using a Bruker amaZon QIT/MS. As with the ion trap at LBNL, the background water pressure is sufficiently high for hydration of unsaturated metal cation complexes prior to, or during, the IRMPD experiments. When hydration was sufficiently fast to yield hydrates of the studied ion and/or its fragments on the timescale of the IRMPD experiments the produced hydrates were continuously ejected from the ion trap to minimize any potential contribution from them to the IRMPD spectra. In addition to the capability for hydration, complexes can be subjected to CID to induce fragmentation followed by IRMPD of the resulting products. The FELIX QIT/MS has been

modified[22,23] such that the high-intensity tunable IR beam from FELIX can be directed into the ion packet, resulting in multiphoton dissociation that is appreciable only when the IR frequency is in resonance with an adequately high-absorption vibrational mode of the particular mass-selected complex being studied. The FEL produces ~5 μs long IR pulses with an energy of typically 40 mJ, which are in the form of a sequence of ~5-ps long micropulses at a 1 GHz repetition rate. An infrared spectrum of the mass isolated ions is obtained by measuring the photodissociation yield as a function of IR laser frequency. This IRMPD approach was previously employed to study crown ether[24,25] and organouranyl complexes.[26]

Computational Methods

The geometry optimizations and vibrational frequency analyses were initial performed with B3LYP hybrid density functional[27,28] by using Gaussian 09 software.[29] The scalar-relativistic Stuttgart energy-consistent pseudopotential with 32-valence-electron and associated ECP60MWB_ANO valence basis set[30,31] were used for the uranium atom, and Dunning's correlation consistent all-electron basis sets with polarized triple-zeta (cc-pVTZ)[32-34] were used for the oxygen, carbon and hydrogen atoms. The geometry optimizations were performed without symmetry restrictions and were followed by vibrational frequency analysis to determine the local minima or saddle point natures of the optimized structures. The reported reaction energies were obtained by combining the electronic energies with the zero-point vibrational energy corrections.

In further electronic structure calculations using PBE functional[35] with ADF code,[36] the scalar-relativistic zeroth-order regular approximation (ZORA)[37,38] was used in conjunction with Slater type orbitals (STOs) of the quality of triple-zeta plus two polarization functions (TZ2P).[39] The bond order analyses based on the Mayer method (BO_{Mayer}),[40] the Gopinathan-Jug indices[41] and Nalewajski-Mrozek method (BO_{NM})[42] were performed. The charge analyses based on Mulliken method, Hirshfeld analysis,[43] Voronoi deformation density,[44] and Multipole derived charges[45] were calculated as well.[46] The energy decomposition analyses (EDA) based on canonical molecular orbitals[47,48] and theoretical analyses via combined extended transition state (ETS) with the natural orbitals for chemical valence (NOCV) theory was carried out.[42,49] The electron localization functions (ELF)[50] were calculated to investigate the feature of the weak dative bonding.

Results and Discussion

Synthesis and Reactivity of Uranyl-12C4 Complexes

The complexes $[UO_2(12C4)_2]^{2+}$and $[UO_2(12C4)_2(OH)]^+$ were abundant in the ESI mass spectra (Fig. S1). The CID mass spectrum of $[UO_2(12C4)_2]^{2+}$ is shown in Figure 1; a dominant process resulted in $[UO_2(12C4\text{-}H)]^+$, reaction (1). CID of $[UO_2(12C4)_2(OH)]^+$ resulted in $[UO_2(12C4)(OH)]^+$, reaction (2), as shown in Figure 2. Spontaneous addition of water to $[UO_2(12C4\text{-}H)]^+$ yielded $[UO_2(12C4\text{-}H)(H_2O)]^+$, reaction (3), as shown in Figure 3. The species tentatively assigned as $[UO_2(12C4)(OH)]^+$ and $[UO_2(12C4\text{-}H)(H_2O)]^+$ have the same compositions. The initial supposition that they have different structures is based on their different reactivities with water. The results for the reaction of $[UO_2(12C4)(OH)]^+$ with background water are shown in Figure 4. Comparison of Figures 3 and 4, which were acquired under the same experimental conditions, reveals that $[UO_2(12C4\text{-}H)(H_2O)]^+$ does not exhibit addition of a second water molecule to yield $[UO_2(12C4\text{-}H)(H_2O)_2]^+$, which would have the same composition as $[UO_2(12C4)(OH)(H_2O)]^+$. In contrast, isomeric $[UO_2(12C4)(OH)]^+$ readily adds a water molecule to yield what is presumed to be the hydrate $[UO_2(12C4)(OH)(H_2O)]^+$. The synthetic approaches, reactions (2) and (3), along with the differing hydration behaviors, suggest the respective assignments of the different isomers as $[UO_2(12C4)(OH)]^+$ from CID reaction (2) and $[UO_2(12C4\text{-}H)(H_2O)]^+$ from water addition reaction (3). To assess this hypothesis, IRMPD spectra were acquired for the two isomers prepared by reactions (2) and (3) and compared with those computed for the two structures, as discussed below. The computed structures of the other uranyl-12C4 complexes were also evaluated by comparison with the experimental IR spectra.

$[UO_2(12C4)_2]^{2+} \rightarrow [UO_2(12C4\text{-}H)]^+ + H12C4^+$ (1) Endothermic CID

$[UO_2(12C4)_2(OH)]^+ \rightarrow [UO_2(12C4)(OH)]^+ + 12C4$ (2) Endothermic CID

$[UO_2(12C4\text{-}H)]^+ + H_2O \rightarrow [UO_2(12C4\text{-}H)(H_2O)]^+$ (3) Spontaneous exothermic

Structures of $[UO_2(12C4)_2]^{2+}$ and $[UO_2(12C4)_2(OH)]^+$

The computed structures of the ground-state (GS) $[UO_2(12C4)_2]^{2+}$ and $[UO_2(12C4)_2(OH)]^+$ cations are shown in Figure 5; selected geometrical parameters are reported in Table 1, with more detailed structural information and a higher-energy isomer provided in

supporting information. The computed $[UO_2(12C4)_2]^{2+}$ ground-state (GS) structure is characterized by *side-on* coordination of the two ligands with the uranium metal center hexa-coordinated by three oxygen atoms from each 12C4 ligand with U-O_{ligand} distances of 2.60 Å, 2.70 Å and 2.77 Å. The fourth U-O_{ligand} distance of greater than 3 Å is too long for a significant bonding interaction. In contrast to the previously reported $[UO_2(15C5)_2]^{2+}$ structure, which was found to have a peculiar equatorial coordination of six oxygen atoms coplanar and non-perpendicular to the uranyl moiety,[17] in $[UO_2(12C4)_2]^{2+}$ the six coordinating oxygen atoms in the 12C4 ligands are not strictly in the so-called equatorial plane, nor are they coplanar. Furthermore, the uranyl moiety is significantly bent from linearity, to 149°, though both U-O distances are 1.740 Å as is typical of uranyl distances. Although in this complex the axial and equatorial orientations significantly depart from typical geometries of linear uranyl coordinated in the equatorial plane, the nature of the complexes, notably the bond distances, indicates an inherently U=O_{yl} and U-O_{eq} type of coordination, where O_{yl} denotes U-O bonding that is characteristic of uranyl, and O_{eq} denotes coordination by oxygen atoms in the quasi-equatorial region around uranium in uranyl. The uranium-oxygen bond lengths (U-O_{yl} is 1.78 Å and average for the six U-O_{eq} is 2.69 Å, Table 1) and overall coordination are comparable to those previously computed for the $[UO_2(15C5)_2]^{2+}$ ion for which U-O_{yl} is 1.74 Å, and an average for the six U-O_{eq} is 2.65 Å.[17] The primary difference between the $[UO_2(12C4)_2]^{2+}$ and $[UO_2(15C5)_2]^{2+}$ structures is the substantial deviation from linearity of the uranyl moiety in the former, coincident with more non-planar coordination of the O_{eq} "equatorial" coordination of the 12C4. The substantial distortion from strictly equatorial coordination is attributed to the more compact and rigid nature of the 12C4 ligand, which precludes near-planar coordination by the crown ether oxygen atoms to uranium.

For $[UO_2(12C4)_2]^{2+}$, an alternative inclusion isomer with a linear uranyl moiety and each of the crown ether ligands cycle about the U-O_{yl} axial bonds with tetra-coordination to the uranium metal center, was found to be significantly higher in energy (+109.4 kcal/mol; see Fig. S5). Although much higher in energy, this structure is remarkable in having two short U=O_{yl} bonds of 1.74 Å and eight short "U-O_{eq}" distances of 2.63 Å to yield a high net uranium-oxygen coordination of 10. Despite this high degree of uranium-oxygen coordination, the high-energy structure is evidently substantially destabilized due to repulsive interactions between the four 12C4 oxygens and the two uranyl oxygens.

The $[UO_2(12C4)_2]^{2+}$ cations were isolated and photofragmented using FELIX to generate IRMPD spectra in the wavelength range of 500 cm^{-1} to 1800 cm^{-1}. The experimental and computed IR spectra for the GS isomer are shown in Figure 6(a); those for the inclusion isomer are shown in Figure S8 (supporting information). A scaling factor of 0.98 was applied to the computed DFT frequencies to account for mode anharmonicities and deficiency in the exchange-correlation functional used.[51-53] As is apparent in Fig. 6(a) there is good agreement between the IRMPD spectra and the computational results for the GS isomer. The computed spectrum for the high-energy structure is not in accord with the experimental spectrum (Fig. S8). These results provide a high level of confidence that the structure of the synthesized species is that computed as the GS structure. The experimental uranyl ν_3 asymmetric stretch mode at 968 cm^{-1} is only slightly less red-shifted than the most extreme previously reported red-shift to 965 cm^{-1} for a dipositive gas-phase uranyl complex,[54] indicating substantial charge donation to the uranyl moiety from the two tridentate oxygen donor 12C4 ligands.

ESI also produced the $[UO_2(12C4)_2(OH)]^+$ complex. The computed GS structure is shown in Figure 5 (selected geometrical parameters are in Table 1). As is apparent in Figure 6(b) there is good agreement between the computed and experimental IR spectra, substantiating the validity of the reported GS structure. The addition of an anionic OH^- group to $[UO_2(12C4)_2]^{2+}$ induces a slight elongation of the $U\text{-}O_{yl}$ bond (from 1.74 to 1.77 Å). This elongation is in accord with additional charge donation, weakening of the $U\text{-}O_{yl}$ bonds, and a resulting further red-shift of the uranyl ν_3 asymmetric stretching mode to 931 cm^{-1}. The steric congestion introduced by the hydroxyl ligand results in reduced coordination of the 12C4 oxygen atoms in $[UO_2(12C4)_2(OH)]^+$. One of the 12C4 ligands exhibits bidentate coordination with $U\text{-}O_{eq}$ distances of 2.60 and 2.77 Å, with the other two $U\text{-}O_{12C4}$ distances being very long (>3.9 Å). The other 12C4 ligand has four relatively long U-O distances in the range of 2.87 – 3.13 Å; the U-O coordination for this second 12C4 ligand is furthermore well outside of the equatorial plane. In accord with the steric congestion in this complex the dominant CID process is loss of one of the two 12C4 ligands, reaction 2, as seen in Figure 2.

The binding mechanisms and strengths of 12C4 ligands to uranyl is of primary interest. To provide insight into uranyl-12C4 interactions, we take $UO_2(12C4)_2^{2+}$ as an example to analyze the electronic structures and metal-ligand bonding. Several chemical bonding analysis methods were used. The results of the energy decomposition analysis (EDA) based on canonical

molecular orbitals for the process UO_2^{2+} + 12C4 → $UO_2(12C4)_2^{2+}$ are given in Table 2. The results show that electrostatic and orbital interactions both contribute to the total bonding energy, which indicates that in addition to electrostatic interactions covalency plays a role in the metal-ligand binding. From analysis using the extended transition state (ETS) method, combined with natural orbitals for chemical valence (ETS-NOCV), the covalent character in $UO_2(12C4)_2^{2+}$ can be understood in terms of the dominant density deformation channels, $\Delta\rho_1(r)$, $\Delta\rho_2(r)$, $\Delta\rho_3(r)$, $\Delta\rho_4(r)$, $\Delta\rho_5(r)$, $\Delta\rho_6(r)$, and $\Delta\rho_7(r)$, which arise from the ligand-to-metal donation as shown in Table 3 and Figure 7. These interactions provide energetic stabilizations of −21.01 kcal/mol (ΔE_{orb1}), −23.53 kcal/mol (ΔE_{orb2}), −15.68 kcal/mol (ΔE_{orb3}), −20.50 kcal/mol (ΔE_{orb4}), −14.80 kcal/mol (ΔE_{orb5}), −8.41 kcal/mol (ΔE_{orb6}), and −12.10 kcal/mol (ΔE_{orb7}). Atomic charge analysis shows that for O_{eq2} atoms the average VDD charges (-0.15, Table 2) are more negative than the O-atom in U-O_{eq1}, for which the average VDD charge on the oxygen atoms is -0.09. This charge difference can be attributed to donation of electrons in the 12C4 ligands to stabilize the U−O_{eq} dative bonds. The value of the electron localization function (ELF, Figure 8) for those six terminal U−O_{eq} bonds are primarily centered on U and O_{eq} atoms, revealing that there is non-negligible covalent interaction between U and O atoms, although the U−O_{eq} bonds are largely ionic in character.

Coordination of uranyl by 12C4 in crystalline solids has revealed that this small outer-sphere crown does not effectively compete with other more strongly coordinating ligands such as water. The result is structures in which the 12C4 exhibits monodentate coordination with only one ethereal oxygen atom coordinating in the equatorial uranyl plane.[55,56] Equatorial coordination of uranyl is completed, for example, by two chloride anions and two water molecules that are hydrogen bonded to additional outer sphere 12C4 ligands. In other crystal structures 12C4 does not whatsoever coordinate uranyl but instead with water forms an organic layer that separates layers of inorganic polymeric chains.[7] The tridentate quasi-equatorial coordination of the two crown ligands in gas-phase $[UO_2(12C4)_2]^{2+}$, and approximately tridentate/bidentate crown coordination in $[UO_2(12C4)_2(OH)]^{+}$, is facilitated in these isolated complexes by the absence of the competitive coordination that dominates in condensed phase.

Structure of $[UO_2(12C4\text{-}H)]^{+}$

As reported above and shown in Figure 1, CID of $[UO_2(12C4)_2]^{2+}$ resulted in $[UO_2(12C4\text{-}H)]^+$ (m/z 445) according to reaction (1). Absent rearrangement, this CID process would result in a radical C atom that could bind to uranium to form an organoactinyl; however, this structure, shown in Figure S6, is 53 kcal/mol above the computed GS structure. The GS structure of $[UO_2(12C4\text{-}H)]^+$, shown in Fig. 5, contains an acyclic (12C4-H) ligand, which wraps around the uranyl moiety, tetra-coordinated in the equatorial plane, and displays U-O_{eq} bond distances that are significantly shorter (i.e. < 2.6 Å) than the values for the complexes described above which comprise intact 12C4 ligands. The structure of the 12C4-H ligand in the GS structure corresponds to cleavage of a C-O bond with elimination of an H atom from 12C4 to yield CH_2=CH-O-CH_2-CH_2-O-CH_2-CH_2-O-CH_2-CH_2-O•. The terminal radical O atom forms a single-bond to the uranium metal center with a short U-O bond distance of 2.09 Å, which is comparable to the U-OH single-bond distance of 2.10 Å reported below. The other three U-O_{eq} bond distances of 2.50, 2.58 and 2.58 Å are much longer and are characteristic of dative coordinate bonds. The U-O_{yl} bond lengths, 1.76-1.77 Å, are comparable to those in $[UO_2(12C4)_2(OH)]^+$ (1.75-1.76 Å), which is an indication of the strong bonding interaction between the single radical oxygen and the UO_2^{2+} moiety; in essence the 12C4-H ligand can be considered as an alkoxide-type anion, in analogy with the OH^- hydroxide ligand. Accordingly, the uranyl ν_3 asymmetric stretching mode (936 cm^{-1}) is significantly lower than the corresponding value for dipositive $[UO_2(12C4)_2]^{2+}$ (968 cm^{-1}) and close to that of $[UO_2(12C4)_2(OH)]^+$ (931 cm^{-1}). In the higher energy (+53 kcal/mol) structural isomer the uranyl moiety departs significantly from linearity (from 180° to 120.7°) and the metal interacts directly with the deprotonated carbon atom of the crown-ether molecule, as well as with all four ether oxygen atoms. This organouranyl complex exhibits a U-C bond length of 2.34 Å, which is comparable to those for previously reported gas-phase organouranyl complexes[26] (Figure S6, supporting information).

As is apparent in Figure 9 there is good agreement between the computed IR spectrum for the GS isomer of $[UO_2(12C4\text{-}H)]^+$and the IRMPD spectra. The computed spectrum for the high energy isomer is shown along with the experimental spectra in Figure S9, where it is seen that the experiment/theory agreement is much less satisfactory. In particular, the rather intense absorption for this isomer around 950 cm^{-1} is not predicted, and the observed absorption around 820 cm^{-1} is much less intense than predicted. Based on comparison of the experimental and computed spectra it can be concluded that the GS structure of $[UO_2(12C4\text{-}H)]^+$ shown in Fig. 5 is

the dominant or sole isomer produced in the experiments. Cleavage of the cyclic 12C4 ligand results in formation of a strong U-O single bond, which is a more energetically favorable scenario than an intact 12C4-H ring with a U-C organouranyl bond. This is a manifestation of the very strong bonds formed between uranium and oxygen.

Structures of Isomers $[UO_2(12C4)(OH)]^+$ and $[UO_2(12C4\text{-}H)(H_2O)]^+$

As noted above (Fig. 2), CID of $[UO_2(12C4)_2(OH)]^+$ resulted in $[UO_2(12C4)(OH)]^+$, which has the same composition as the alternative hydrate structure, $[UO_2(12C4\text{-}H)(H_2O)]^+$. The CID product of reaction (2) is speculated to be $[UO_2(12C4)(OH)]^+$ because this would result from elimination of a 12C4 ligand without any rearrangement, an assumption that may well be invalid under CID conditions. Gas-phase addition of water to $[UO_2(12C4\text{-}H)]^+$, produced by CID of $[UO_2(12C4)_2(OH)]^+$ as described above, yielded what is tentatively assigned as the hydrate, $[UO_2(12C4\text{-}H)(H_2O)]^+$, reaction (3). The postulated formation of the alternative hydroxide and hydrate structures are given by endothermic CID reaction (2) and spontaneous exothermic hydration reaction (3).

The GS structures of the hydroxide and hydrate isomers, $[UO_2(12C4)(OH)]^+$ and $[UO_2(12C4\text{-}H)(H_2O)]^+$, are shown in Figure 5; substantially higher energy (>50 kcal/mol) structures for both the hydroxide and hydrate isomers are shown in Figure S7. The GS $[UO_2(12C4)(OH)]^+$ structure is computed to be 25.8 kcal/mol higher energy than GS $[UO_2(12C4\text{-}H)(H_2O)]^+$, such that based on energetics alone the products of both reactions (2) and (3) would be assigned as the hydrate, not the hydroxide as proposed in CID reaction (2). Referring to Figures 3 and 4, it is apparent that the reactivity of the isomers produced by reaction (2) and reaction (3) are substantially different. The $[UO_2(12C4\text{-}H)]^+$ complex efficiently adds water to yield what is postulated has the hydrate $[UO_2(12C4\text{-}H)(H_2O)]^+$. The $[UO_2(12C4)(OH)]^+$ complex, which has the same composition as the hydrate very efficiently adds water to yield what is proposed to be the hydroxide hydrate $[UO_2(12C4)(OH)(H_2O)]^+$, a process that is nearly complete within 0.1 second under these experimental conditions. If $[UO_2(12C4\text{-}H)(H_2O)]^+$ were actually the hydroxide then the hydrate would be apparent in Figure 3; the absence of a peak in Figure 3 corresponding to addition of a second water molecule indicates that the first water addition product does not have the same structure as the isomer identified as $[UO_2(12C4)(OH)]^+$ in Figure 4.

The water addition chemistry evident in Figures 3 and 4 suggests that the two isomers are $[UO_2(12C4\text{-}H)(H_2O)]^+$ and $[UO_2(12C4)(OH)]^+$. Referring to the structures in Figure 5, it is apparent that the $[UO_2(12C4)(OH)]^+$ isomer has a largely exposed uranium metal center that might enable facile hydration. In contrast, the $[UO_2(12C4\text{-}H)(H_2O)]^+$ isomer is essentially uranyl with pentacoordination in the equatorial plane, a configuration that is not amenable to addition to further hydration. Similarly, the highly coordinated uranium centers in $[UO_2(12C4)_2]^{2+}$ and $[UO_2(12C4)_2(OH)]^+$ (Fig. 5) render these species resistant to hydration, as seen in Figures S3 and S4.

IRMPD spectra acquired for the species with the same composition but produced by reactions (2) and (3) are shown in Figure 10. It is readily apparent that the species produced by reaction (2) (black spectrum in Fig. 10a) and that produced by reaction (3) (black spectrum in Fig. 10b) are very different, indicating different structures for these two species with the same composition, as postulated above. From Figure 10a it is apparent that the complex provisionally assigned as $[UO_2(12C4)(OH)]^+$ from reaction (2) does indeed exhibit an IRMPD spectrum in good agreement with that computed for the GS structure of this hydroxide species. Similarly, Figure 10b reveals good agreement between the hydrate complex proposed from reaction (3) and the computed spectrum for this species. Comparison of the IRMPD spectra with the computed high-energy isomers of the hydroxide and hydrate complexes, shown in Figure S10, reveal poor correspondences.

The comparisons of the IRMPD and computed IR spectra reveal that the hypotheses presented above, and summarized as reactions (2) and (3) are valid. Although the hydroxide structure is substantially (ca. 26 kcal/mol) higher in energy than the hydrate structure, CID elimination of a 12C4 ligand from $[UO_2(12C4)_2(OH)]^+$ results in retention of the hydroxyl ligand rather than abstraction of a H atom from the 12C4 ligand to yield the lower-energy hydrate. The GS structure of $[UO_2(12C4\text{-}H)(H_2O)]^+$ (Figure 5) is similar to that of $[UO_2(12C4\text{-}H)]^+$ with the H_2O molecule equatorially coordinating the partially exposed uranium metal center and providing equatorial coordination by five O atoms. Conversion of the hydroxide to the more stable hydrate would require C-O bond cleavage of the intact 12C4 ligand, which evidently does not occur upon CID elimination of a 12C4 ligand from $[UO_2(12C4)_2(OH)]^+$. Addition of H_2O to $[UO_2(12C4\text{-}H)]^+$ retains the cleaved 12C4-H ligand to yield the most stable hydrate structure.

The GS $[UO_2(12C4)(OH)]^+$ complex produced by loss of a 12C4 ligand via reaction 2 can be represented as $[UO_2(OH)]^+$ coordinated by a 12C4 ligand (Figure 5). In contrast to bare $[UO_2(OH)]^+$, in the complex this unit has a non-planar structure with a $O_{yl}UO_{OH}$-O_{yl} dihedral angle of ca. 150°, where the dihedral angle is that which atom O_{yl} makes with respect to the plane defined by the first three atoms O_{yl},U,O_{OH}. The non-planar uranyl hydroxide unit is coordinated by the 12C4 ligand in a side-on manner with U-O bond lengths of > 2.6 Å. Both U-O_{yl} bond lengths are significantly elongated relative to the other uranyl complexes, to ca 1.77 Å, and the uranyl moiety significantly deviates from linearity to ca. 150°. This geometry allows hydration of this isomeric structure.

Conclusions

Gas-phase uranyl–(12-Crown-4) complexes $[UO_2(12C4)_2]^{2+}$ and $[UO_2(12C4)_2(OH)]^+$ were prepared by ESI. CID of the dication yielded $[UO_2(12C4\text{-}H)]^+$ in which the 12C4 ring is cleaved to produce a strong U-O_{ligand} single bond. The structure of the isomer produced by water addition to the latter was confirmed as the hydrate $[UO_2(12C4\text{-}H)(H_2O)]^+$ whereas the isomer produced by CID elimination of 12C4 from $[UO_2(12C4)_2(OH)]^+$ was confirmed as the hydroxide $[UO_2(12C4)(OH)]^+$. Although the hydroxide isomer is 26 kcal/mol higher in energy it does not rearrange via cleavage of the 12C4 ring to form the lower-energy hydrate. The gas-phase chemistry of the two isomers indicated the postulated structures, which were confirmed by comparison of the IRMPD spectra with the computed IR spectra. The results provide a clear example of the formation of distinct isomers in the gas phase by using different synthetic routes and also the utility of IRMPD spectroscopy combined with DFT computations to confirm isomeric structures. The computed structures of the uranyl-12C4 complexes, which were confirmed by IRMPD, exhibit a variety of bonding of the uranium to 12C4, in some cases with resulting substantial distortions of the uranyl moiety to accommodate high-coordination by the small and rigid 12C4 (or 12C4-H) ligand(s). These results help to understand the interaction between Uranyl and crown ethers with varying size.

Supporting Information

ESI mass spectrum of the uranyl/12C4 solution. CID mass spectrum of $(12C4)H^+$. Mass spectra of $[UO_2(12C4)_2(OH)]^+$ and $[UO_2(12C4)_2]^{2+}$ after isolation, showing no water-addition. Optimized

structures of higher-energy isomers of $[UO_2(12C4)_2]^{2+}$, $[UO_2(12C4\text{-}H)]^{+}$, $[UO_2(12C4\text{-}H)(H_2O)]^{+}$, and $[UO_2(12C4)(OH)]^{+}$. Comparison between the obtained IRMPD spectra and computed IR spectra of high-energy isomers of $[UO_2(12C4)_2]^{2+}$, $[UO_2(12C4\text{-}H)]^{+}$, $[UO_2(12C4\text{-}H)(H_2O)]^{+}$, and $[UO_2(12C4)(OH)]^{+}$.

Acknowledgements

Research was supported by the Center for Actinide Science and Technology, an Energy Frontier Research Center funded by the U.S. Department of Energy, Office of Science, Basic Energy Sciences, under Award Number DE-SC0016568 [J.K.G.]; by start-up funds from the Bayer School of Natural and Environmental Sciences and Duquesne University [M.V.S.]; and by the Netherlands Organisation for Scientific Research (NWO) under vici-grant no. 724.011.002 and the Stichting Physica [J.O.]. We gratefully acknowledge NWO for the support of the FELIX Laboratory. The computational work was financially supported by the Science Challenge Project (No. JCKY2016212A504) and by the National Natural Science Foundation of China (NSFC Nos. 91426302, 21433005) of China [J.L.] and by the NSFC (No. 21701006) [S.X.H]. The calculations were performed at the Supercomputer Center of the Computer Network Information Center, Chinese Academy of Sciences and Tsinghua National Laboratory for Information Science and Technology, China.

Keywords: Uranyl 12-Crown-4 Complex • Electronic Structure • DFT• Infrared spectroscopy

References

(1) Alexander, V.: Design and Synthesis of Macrocyclic Ligands and Their Complexes of Lanthanides and Actinides. *Chemical Reviews* **1995**, *95*, 273-342.

(2) Gorden, A. E. V.; Xu, J.; Raymond, K. N.; Durbin, P.: Rational Design of Sequestering Agents for Plutonium and Other Actinides. *Chemical Reviews* **2003**, *103*, 4207-4282.

(3) Hudson, M. J.; Harwood, L. M.; Laventine, D. M.; Lewis, F. W.: Use of Soft Heterocyclic N-Donor Ligands To Separate Actinides and

Lanthanides. *Inorganic Chemistry* **2012**, *52*, 3414-3428.

(4) Gokel, G. W.; Leevy, W. M.; Weber, M. E.: Crown ethers: Sensors for ions and molecular scaffolds for materials and biological models. *Chemical Reviews* **2004**, *104*, 2723-2750.

(5) Pedersen, C. J.; Frensdor, H. K.: Macrocyclic Polyethers and Their Complexes. *Angewandte Chemie-International Edition* **1972**, *11*, 16-&.

(6) Cooper, T. E.; Carl, D. R.; Oomens, J.; Steill, J. D.; Armentrout, P. B.: Infrared Spectroscopy of Divalent Zinc and Cadmium Crown Ether Systems. *Journal of Physical Chemistry A* **2011**, *115*, 5408-5422.

(7) Rogers, R. D.; Bond, A. H.; Hipple, W. G.; Rollins, A. N.; Henry, R. F.: Synthesis and Structural Elucidation of Novel Uranyl Crown-Ether Compounds Isolated from Nitric, Hydrochloric, Sulfuric, and Acetic-Acids. *Inorganic Chemistry* **1991**, *30*, 2671-2679.

(8) Rogers, R. D.; Kurihara, L. K.; Benning, M. M.: F-Element Crown Ether Complexes .9. The Role of Solvent Hydrogen-Bonding - Synthesis and Crystal-Structure of Aquatetrachlorotris(Ethanol)Thorium(IV)-1,4,7,10,13,16-Hexaoxacyclo-Octadecane Water (1/1/1). *Journal of the Chemical Society-Dalton Transactions* **1988**, 13-16.

(9) Rogers, R. D.; Kurihara, L. K.; Benning, M. M.: F-Element Crown-Ether Complexes .11. Preparation and Structural Characterization of $[UO_2(OH2)_5]$ $[ClO_4]$2.3(15-Crown-5).CH_3CN and$[UO_2(OH2)_5]$ $[ClO_4]$2.3(18-Crown-6).$CH_3CN.H_2O$. *Journal of Inclusion Phenomena* **1987**, *5*, 645-658.

(10) Eller, P. G.; Penneman, R. A.: Synthesis and Structure of 1-1 Uranyl-Nitrate Tetrahydrate-18-Crown-6 Compound, $UO_2(NO_3)_2(H_2O)_2.2H_2O$.(18-Crown-6) - Non-Coordination of Uranyl by Crown Ether. *Inorganic Chemistry* **1976**, *15*, 2439-2442.

(11) Navaza, A.; Villain, F.; Charpin, P.: Crystal-Structures of the Dicyclohexyl-(18-Crown-6) Uranyl Perchlorate Complex and of Its Hydrolysis Product. *Polyhedron* **1984**, *3*, 143-149.

(12) Deshayes, L.; Keller, N.; Lance, M.; Navaza, A.; Nierlich, M.; Vigner, J.: EXAFS Analysis of Aqueous and Acetonitrile Solutions of UO_2-Triflate with Crown-Ethers and Aza-Crowns - Crystals Structures of the Inclusion Complexes UO_2(18-Crown-6)$(CF_3SO_3)_2$ and UO_2(Dicyclohexyl-18-Crown-6)$(CF_3SO_3)_2$. *Polyhedron* **1994**, *13*, 1725-1733.

(13) Servaes, K.; De Houwer, S.; Görller-Walrand, C.; Binnemans, K.: Spectroscopic properties of uranyl crown ether complexes in non-aqueous solvents. *Physical Chemistry Chemical Physics* **2004**, *6*, 2946-2950.

(14) Clark, D. L.; Keogh, D. W.; Palmer, P. D.; Scott, B. L.; Tait, C. D.: Synthesis and structure of the first transuranium crown ether inclusion complex: [NpO2([18]crown-6)]ClO4. *Angewandte Chemie-International Edition* **1998**, *37*, 164-166.

(15) Shamov, G. A.; Schreckenbach, G.; Martin, R. L.; Hay, P. J.: Crown ether inclusion complexes of the early actinide elements, [AnO(2)(18-crown-6)](n+), An = U, Np, Pu and n=1, 2: A relativistic density functional study. *Inorganic Chemistry* **2008**, *47*, 1465-1475.

(16) Gong, Y.; Gibson, J. K.: Crown ether complexes of uranyl, neptunyl, and plutonyl: Hydration differentiates inclusion versus outer coordination. *Inorganic Chemistry* **2014**, *53*, 5839−5844.

(17) Hu, S.-X.; Gibson, J. K.; Li, W.-L.; van Stipdonk, M. J.; Martens, J.; Berden, G.; Redlich, B.; Oomens, J.; Li, J.: Electronic structure and characterization of a uranyl di-15-crown-5 complex with an unprecedented sandwich structure *Chemical Communications* **2016**, *52*, 12761-12764.

(18) Rios, D.; Michelini, M. C.; Lucena, A. F.; Marçalo, J.; Bray, T. H.; Gibson, J. K.: Gas-Phase Uranyl, Neptunyl, and Plutonyl: Hydration and Oxidation Studied by Experiment and Theory. *Inorganic Chemistry* **2012**, *51*, 6603-6614.

(19) Gong, Y.; Hu, H. S.; Tian, G. X.; Rao, L. F.; Li, J.; Gibson, J. K.: A Tetrapositive Metal Ion in the Gas Phase: Thorium(IV) Coordinated by Neutral Tridentate Ligands. *Angewandte Chemie-International Edition* **2013**, *52*, 6885-6888.

(20) Rutkowski, P. X.; Rios, D.; Gibson, J. K.; Van Stipdonk, M. J.: Gas-Phase Coordination Complexes of $U^{VI}O_2^{2+}$, $Np^{VI}O_2^{2+}$, and $Pu^{VI}O_2^{2+}$ with Dimethylformamide. *Journal of the American Society for Mass Spectrometry* **2011**, *22*, 2042-2048.

(21) Oepts, D.; van der Meer, A. F. G.; van Amersfoort, P. W.: The free-electron Laser user facility FELIX. *Infrared Physics and Technology* **1995**, *36*, 297−308.

(22) Martens, J.; Berden, G.; Gebhardt, C. R.; Oomens, J.: Infrared ion spectroscopy in a modified quadrupole ion trap mass spectrometer at the FELIX free electron laser laboratory. *Review of Scientific Instruments* **2016**, *87*, 103108.

(23) Martens, J.; Grzetic, J.; Berden, G.; Oomens, J.: Structural identification of electron transfer dissociation products in mass spectrometry using infrared ion spectroscopy. *Nature Communications* **2016**, *7*, 11754.

(24) Gamez, F.; Hurtado, P.; Martinez-Haya, B.; Berden, G.; Oomens, J.: Vibrational study of isolated 18-crown-6 ether complexes with alkaline-earth metal cations. *International Journal of Mass Spectrometry* **2011**, *308*, 217-224.

(25) Gamez, F.; Hurtado, P.; Hamad, S.; Martinez-Haya, B.; Berden, G.; Oomens, J.: Tweezer-like Complexes of Crown Ethers with Divalent Metals: Probing Cation-Size-Dependent Conformations by Vibrational Spectroscopy in the Gas Phase. *Chempluschem* **2012**, *77*, 118-123.

(26) Dau, P. D.; Rios, D.; Gong, Y.; Michelini, M. C.; Marçalo, J.; Shuh, D. K.; Mogannam, M.; Van Stipdonk, M. J.; Corcovilos, T. A.; Martens, J. K.; Oomens, J.; Berden, G.; Redlich, B.; Gibson, J. K.: Synthesis and hydrolysis of uranyl, neptunyl and plutonyl gas–phase complexes exhibiting discrete actinide–carbon bonds. *Organometallics* **2016**, *25*, 1228–1240.

(27) Becke, A. D.: Density-Functional Thermochemistry .3. The Role of Exact Exchange. *Journal of Chemical Physics* **1993**, *98*, 5648-5652.

(28) Lee, C. T.; Yang, W. T.; Parr, R. G.: Development of the Colle-Salvetti Correlation-Energy Formula into a Functional of the Electron-Density. *Physical Review B* **1988**, *37*, 785-789.

(29) Frisch, M. J.; Trucks, G. W.; Schlegel, H. B.; Scuseria, G. E.; Robb, M. A.; Cheeseman, J. R.; Scalmani, G.; Barone, V.; Mennucci, B.; Petersson, G. A.; Nakatsuji, H.; Caricato, M.; Li, X.; Hratchian, H. P.; Izmaylov, A. F.; Bloino, J.; Zheng, G.; Sonnenberg, J. L.; Hada, M.; Ehara, M.; Toyota, K.; Fukuda, R.; Hasegawa, J.; Ishida, M.; Nakajima, T.; Honda, Y.; Kitao, O.; Nakai, H.; Vreven, T.; Montgomery, J., J.; Peralta, J. E.; Ogliaro, F.; Bearpark, M.; Heyd, J. J.; Brothers, E.; Kudin, K. N.; Staroverov, V. N.; Keith, T.; Kobayashi, R.; Normand, J.; Raghavachari, K.; Rendell, A.; Burant, J. C.; Iyengar, S. S.; Tomasi, J.; Cossi, M.; Rega, N.; Millam, J. M.; Klene, M.; Knox, J. E.; Cross, J. B.; Bakken, V.; Adamo, C.; Jaramillo, J.; Gomperts, R.; Stratmann, R. E.; Yazyev, O.; Austin, A. J.; Cammi, R.; Pomelli, C.; Ochterski, J. W.; Martin, R. L.; Morokuma, K.; Zakrzewski, V. G.; Voth, G. A.; Salvador, P.; Dannenberg, J. J.; Dapprich, S.; Daniels, A. D.; Farkas, Ö.; Foresman, J. B.; Ortiz, J. V.; Cioslowski, J.; Fox, D. J.: Gaussian 09, Revision C.01. Gaussian, Inc.: Wallingford, CT, 2010.

(30) Cao, X. Y.; Dolg, M.; Stoll, H.: Valence basis sets for relativistic energy-consistent small-core actinide pseudopotentials. *Journal of Chemical Physics* **2003**, *118*, 487-496.

(31) Cao, X. Y.; Dolg, M.: Segmented contraction scheme for small-core actinide pseudopotential basis sets. *Journal of Molecular Structure-Theochem* **2004**, *673*, 203-209.

(32) Mclean, A. D.; Chandler, G. S.: Contracted Gaussian-Basis Sets for Molecular Calculations .1. 2nd Row Atoms, Z=11-18. *Journal of Chemical Physics* **1980**, *72*, 5639-5648.

(33) Kendall, R. A.; Dunning, T. H.; Harrison, R. J.: Electron-Affinities of the 1st-Row Atoms Revisited - Systematic Basis-Sets and Wave-Functions. *Journal of Chemical Physics* **1992**, *96*, 6796-6806.

(34) Woon, D. E.; Dunning, T. H.: Gaussian-Basis Sets for Use in Correlated Molecular Calculations .3. The Atoms Aluminum through Argon. *Journal of Chemical Physics* **1993**, *98*, 1358-1371.

(35) Ernzerhof, M.; Perdew, J. P.; Burke, K.: Density functionals: Where do they come from, why do they work? *Density Functional Theory I* **1996**, *180*, 1-30.

(36) Baerends, E. J.; Branchadell, V.; Sodupe, M.: Atomic reference energies for density functional calculations. *Chemical Physics Letters* **1997**, *265*, 481-489.

(37) van Lenthe, E.; Baerends, E. J.; Snijders, J. G.: Relativistic Regular 2-Component Hamiltonians. *Journal of Chemical Physics* **1993**, *99*, 4597-4610.

(38) van Lenthe, E.; Ehlers, A.; Baerends, E. J.: Geometry optimizations in the zero order regular approximation for relativistic effects. *Journal of Chemical Physics* **1999**, *110*, 8943-8953.

(39) van Lenthe, E.; Baerends, E. J.: Optimized slater-type basis sets for the elements 1-118. *Journal of Computational Chemistry* **2003**, *24*, 1142-1156.

(40) Mayer, I.: Charge, Bond Order and Valence in the Abinitio SCF Theory. *Chemical Physics Letters* **1983**, *97*, 270-274.

(41) Gopinathan, M. S.; Jug, K.: Valency .1. A Quantum Chemical Definition and Properties. *Theoretica Chimica Acta* **1983**, *63*, 497-509.

(42) Michalak, A.; DeKock, R. L.; Ziegler, T.: Bond multiplicity in transition-metal complexes: Applications of two-electron valence indices. *Journal of Physical Chemistry A* **2008**, *112*, 7256-7263.

(43) Hirshfeld, F. L.: Bonded-Atom Fragments for Describing Molecular Charge-Densities. *Theoretica Chimica Acta* **1977**, *44*, 129-138.

(44) Bickelhaupt, F. M.; Hommes, N. J. R. V.; Guerra, C. F.; Baerends, E. J.: The carbon-lithium electron pair bond in (CH3Li)(n) (n=1, 2, 4). *Organometallics* **1996**, *15*, 2923-2931.

(45) Swart, M.; Van Duijnen, P. T.; Snijders, J. G.: A charge analysis derived from an atomic multipole expansion. *Journal of Computational Chemistry* **2001**, *22*, 79-88.

(46) Mulliken, R. S.: Electronic Population Analysis on Lcao-Mo Molecular Wave Functions .1. *Journal of Chemical Physics* **1955**, *23*, 1833-1840.

(47) Ziegler, T.; Rauk, A.: Calculation of Bonding Energies by Hartree-Fock Slater Method .1. Transition-State Method. *Theoretica Chimica Acta* **1977**, *46*, 1-10.

(48) Ziegler, T.; Rauk, A.: Theoretical-Study of the Ethylene-Metal Bond in Complexes between Cu+, Ag+, Au+, Pt-0, or Pt-2+ and Ethylene, Based on the Hartree-Fock-Slater Transition-State Method. *Inorganic Chemistry* **1979**, *18*, 1558-1565.

(49) Nalewajski, R. F.; Mrozek, J.; Michalak, A.: Two-electron valence indices from the Kohn-Sham orbitals. *International Journal of Quantum Chemistry* **1997**, *61*, 589-601.

(50) Becke, A. D.; Edgecombe, K. E.: A Simple Measure of Electron Localization in Atomic and Molecular-Systems. *Journal of Chemical Physics* **1990**, *92*, 5397-5403.

(51) Banisaukas, J.; Szczepanski, J.; Eyler, J.; Vala, M.; Hirata, S.; Head-Gordon, M.; Oomens, J.; Meijer, G.; von Helden, G.: Vibrational and Electronic Spectroscopy of Acenaphthylene and its Cation. *Journal of Physical Chemistry A* **2003**, *107*, 782-793.

(52) Merrick, J. P.; Moran, D.; Radom, L.: An Evaluation of Harmonic Vibrational Frequency Scale Factors. *Journal of Physical Chemistry A* **2007**, *111*, 11683-11700.

(53) Groenewold, G.; Van Stipdonk, M. J.; Oomens, J.; de Jong, W. A.; Gresham, G.; McIlwain, M. E.: Vibrational Spectra of discrete UO_2^{2+} halide complexes in the gas phase. *International Journal of Mass Spectrometry* **2010**, *297*, 67-75.

(54) Gibson, J. K.; Hu, H. S.; Van Stipdonk, M. J.; Berden, G.; Oomens, J.; Li, J.: Infrared Multiphoton Dissociation Spectroscopy of a Gas-Phase Complex of Uranyl and 3-Oxa-Glutaramide: An Extreme Red-Shift of the [O=U=O](2+) Asymmetric Stretch. *Journal of Physical Chemistry A* **2015**, *119*, 3366-3374.

(55) Rogers, R. D.; Benning, M. M.; Etzenhouser, R. D.; Rollins, A. N.: Novel Unidentate Coordination of a Crown Ether and of a Polyethylene-Glycol to Uranium(VI). *Journal of the Chemical Society-Chemical Communications* **1989**, 1586-1588.

(56) Rogers, R. D.; Benning, M. M.; Etzenhouser, R. D.; Rollins, A. N.: Synthesis and Structural Characterization of the Monodentate 12-Crown-4 and Hexaethylene Glycol Complexes of Uranium(VI) - [UO2Cl2(OH2)2(12-Crown-4)].12-Crown-4 and UO2Cl2(OH2)2(Hexaethylene Glycol). *Journal of Coordination Chemistry* **1992**, *26*, 299-311.

Table 1. Geometrical parameters (bond lengths in Å and uranyl bond angles in degrees) at B3LYP/ECP60MWB_ANO (U):cc-pVTZ (C, H, O) level of theory. Relative energies (ΔE in kcal/mol) are computed with respect to the ground-state (GS) isomer; vibrational frequencies ν_3 are in cm^{-1}.[a]

	$[UO_2(12C4)_2]^{2+}$		$[UO_2(12C4)_2(OH)]^+$	$[UO_2(12C4\text{-}H)]^+$		$[UO_2(12C4\text{-}H)(H_2O)]^+$		$[UO_2(12C4)(OH)]^+$	
	Side-on **GS**	Insertion	**GS**	Insertion **GS**	Side-on Organo-uranyl[d]	Insertion **GS**	Side-on	Side-on **GS**	Insertion
$U\text{-}O_{yl}$	1.740 1.740	1.739 1.739	1.766 1.746	1.762 1.769	1.792 1.808	1.766 1.771	1.792 1.812	1.765 1.768	1.773 1.780
$U\text{-}O(H/H_2)$	-	-	2.113	-	-	2.533	2.514	2.081	2.096
$U\text{-}O_{eq}$ [b]	2.687 [6]	2.625 [6]	2.981 [4]	2.440 [4]	2.578 [4]	2.482 [4]	2.635 [4]	2.778 [4]	2.553 [4]
$O_{yl}\text{-}U\text{-}O_{yl}$	148.8	180.0	169.2	172.0	120.7	171.3	129.3	149.5	151.8
ΔE	0.0	109.4	0.0	0.0	53.0	0.0	53.8	0.0	66.5
ν_3 Computed[c]	958	954	943	913	868	925	858	906	962
ν_3 IRMPD	968	-	931	936	-	938	-	936	--

[a] Ground-state (GS) optimized structures are reported in Figure 5; the optimized structures of higher-energy isomers are shown in Supporting Information. [b] Average of $U\text{-}O_{eq}$ distances that are less than 3 Å; the number of such $U\text{-}O_{eq}$ interactions is in brackets. [c] Scaling factor 0.98. [d] The U-C distance is 2.390 Å.

Table 2. EDA and ETS-NOCV analysis of $UO_2^{2+} + (12C4)_2 \rightarrow UO_2(12C4)_2^{2+}$ at PBE/TZ2P.

	Inter. Frag: $UO_2(12C4)_2^{2+}$ (^1A) [UO_2^{2+} ($^1\Sigma$); 12C4 (^1A)]			
EDA	ΔE_{orb}	ΔE_{Pauli}	ΔE_{elstat}	ΔE_{int}
	-202.66	128.65	-206.7	-280.7
ETS-NOCV	*i*	$\Delta\rho^i$		ΔE^i_{orb}
	ΔE_1	0.46		-21.01
	ΔE_2	0.46		-23.53
	ΔE_3	0.41		-15.68
	ΔE_4	0.37		-20.50
	ΔE_5	0.35		-14.80
	ΔE_6	0.30		-8.41
	ΔE_7	0.26		-12.10
	ΔE(total)			-185.78
	ΔE(rest)			-36.43

Table 3. Average bond distance and bond order of six terminal U-O_{eq1} bonds, two long U-O_{eq2} and two U-O_{yl} bonds, and average charges of O_{eq} and O_{yl} for $UO_2(12C4)_2^{2+}$ at PBE/TZ2P.

	Distance, Å	Bond Order				
		Mayer	G-J	N-M1	N-M2	N-M3
U-O_{eq1}	2.69	0.32	0.36	0.43	0.72	0.44
U-O_{eq2}	3.48	0.07	0.07	0.08	0.23	0.09
U-O_{yl}	1.78	2.00	2.49	2.84	2.84	2.77
Charge						
	Mulliken	Hirshfeld	VDD	MDC-q		
q(U)	2.35	0.81	0.52	2.55		
q(O_{yl})	-0.58	-0.24	-0.26	-0.63		
q(O_{eq1})	-0.63	-0.09	-0.09	-0.46		
q(O_{eq2})	-0.70	-0.15	-0.15	-0.59		

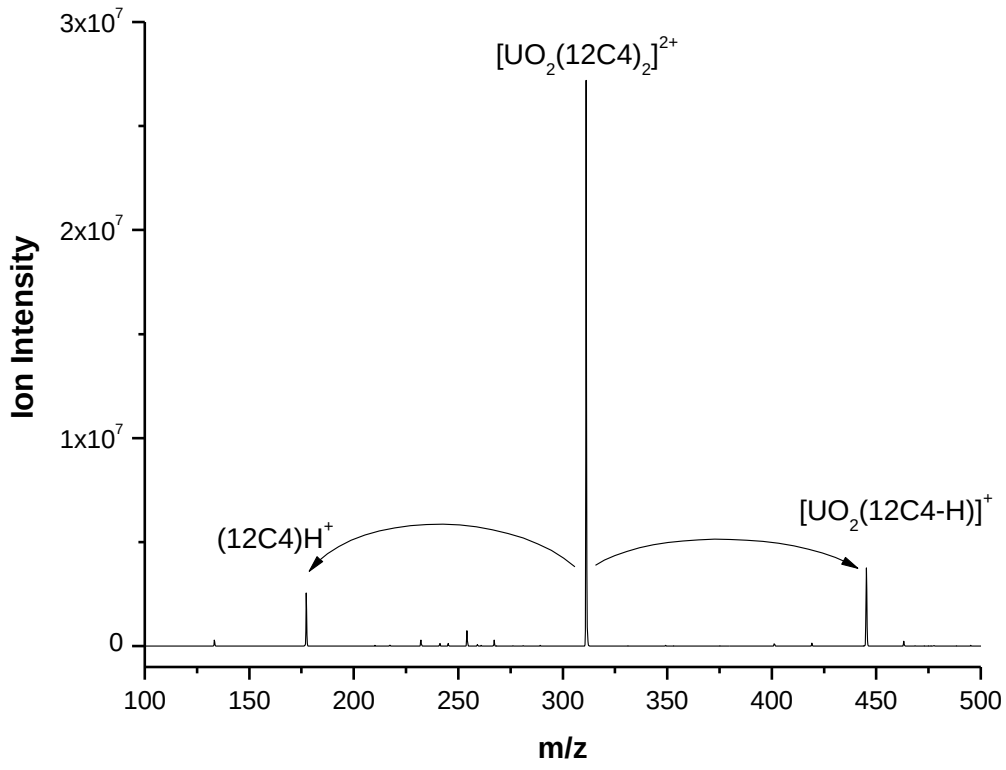

Figure 1. CID mass spectrum of $[UO_2(12C4)_2^{2+}]$ produced by ESI.

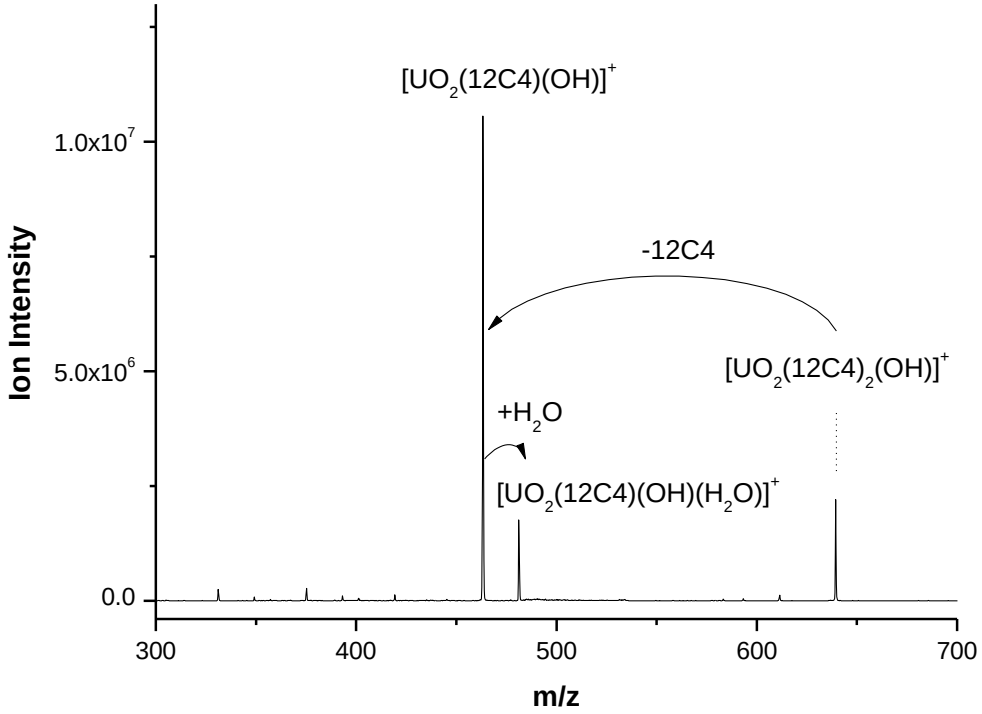

Figure 2. CID mass spectrum of $[UO_2(12C4)_2(OH)]^+$ produced by ESI.

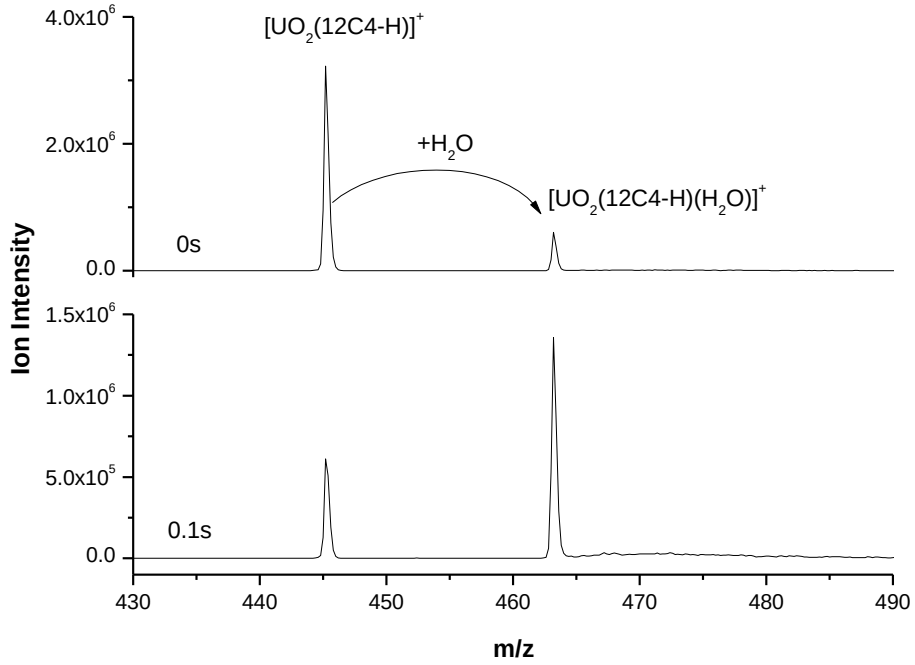

Figure 3. Spontaneous reaction of $[UO_2(12C4\text{-}H)]^+$ with background water for applied times of 0 s and 0.1 s. The reaction product at t = 0 s reflects the inherent time delay before the applied reaction time.

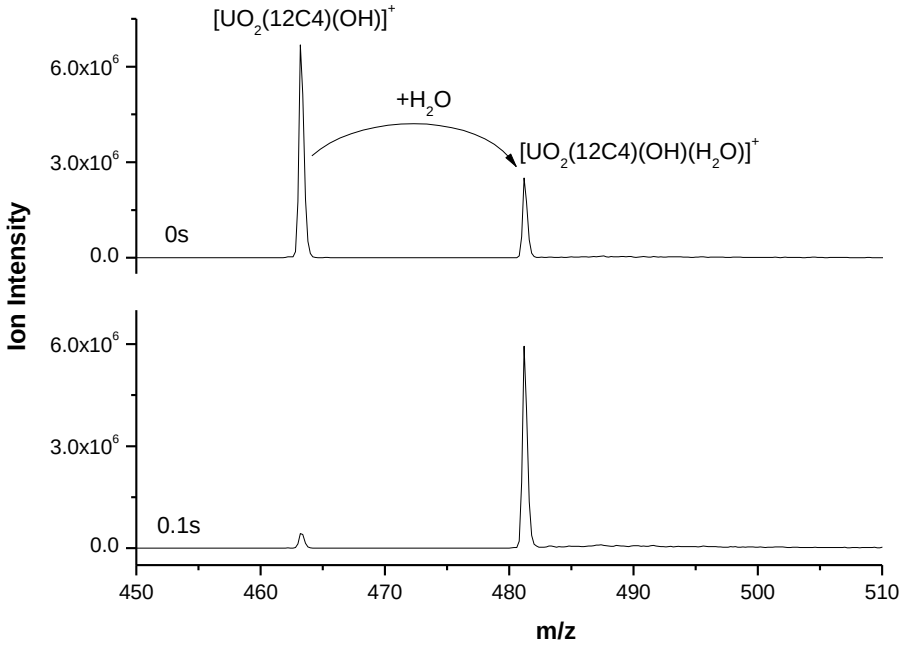

Figure 4. Spontaneous reaction of $[UO_2(12C4)(OH)]^+$ with background water for applied times of 0 s and 0.1 s.

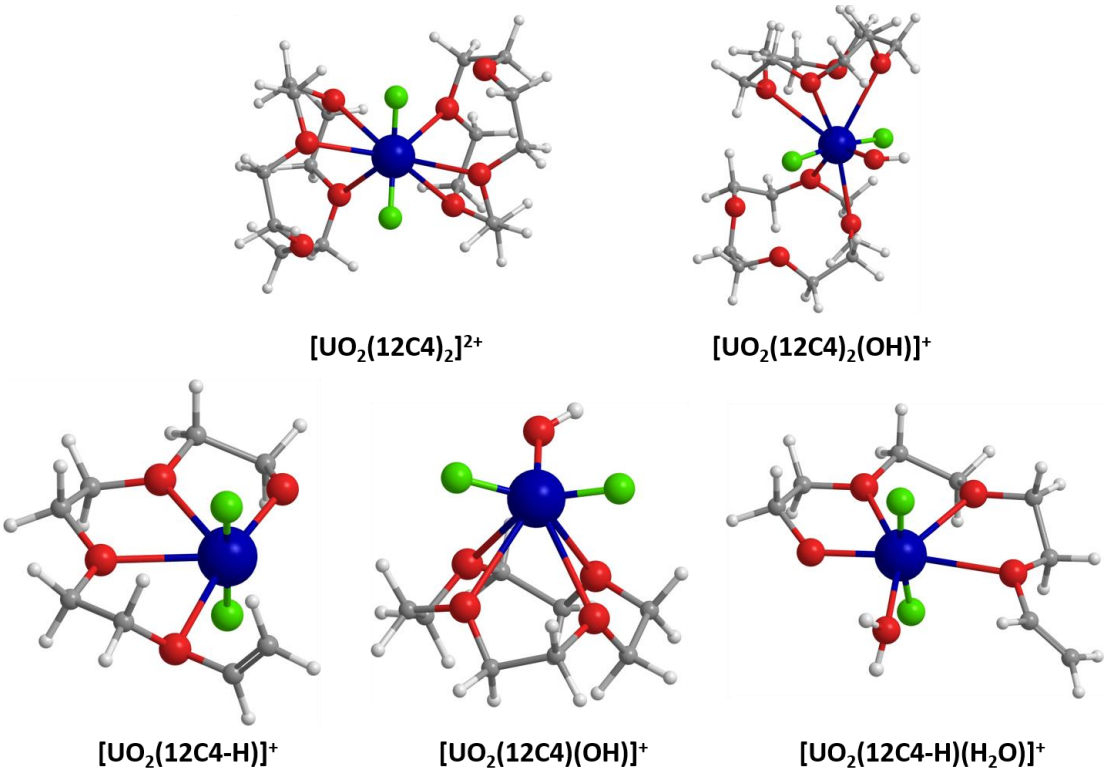

Figure 5. Computed structures of the ground-state $[UO_2(12C4)_2]^{2+}$, $[UO_2(12C4)_2(OH)]^{+}$, $[UO_2(12C4\text{-}H)]^{+}$, $[UO_2(12C4\text{-}H)(H_2O)]^{+}$ and $[UO_2(12C4)(OH)]^{+}$ complexes. Selected geometrical parameters are reported in Table 1. The uranyl O atoms are green while the other O atoms are red.

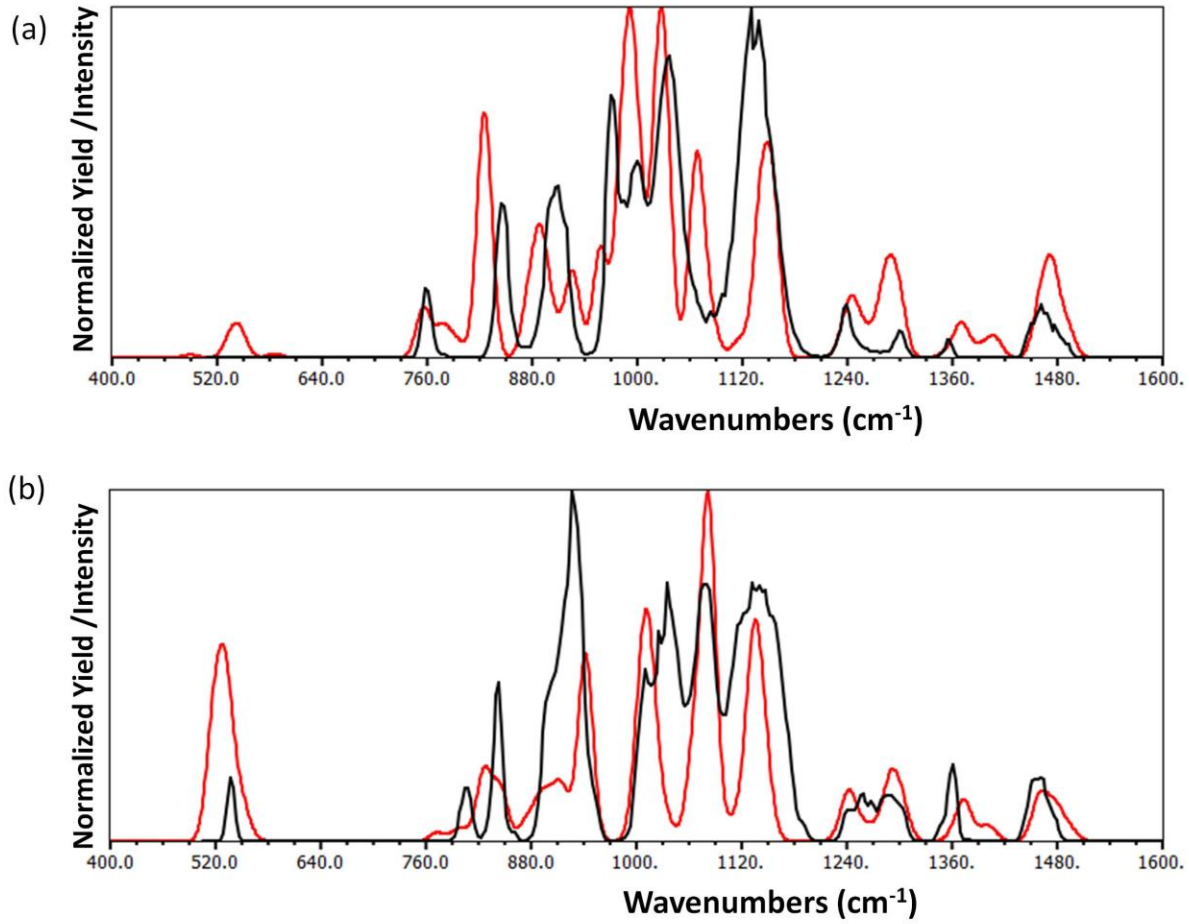

Figure 6. IRMPD spectra of (a) $[UO_2(12C4)_2]^{2+}$ and (b) $[UO_2(12C4)_2(OH)]^{+}$ are in black. In red are the computed IR spectra for the GS structures. Harmonic frequencies for this and the other calculated spectra were computed at the B3LYP/ECP60MWB_ANO (U):cc-pVTZ(C, H, O) level of theory, scaled by a factor of 0.98 and convoluted with a 10 cm^{-1} fwhm Gaussian lineshape function.

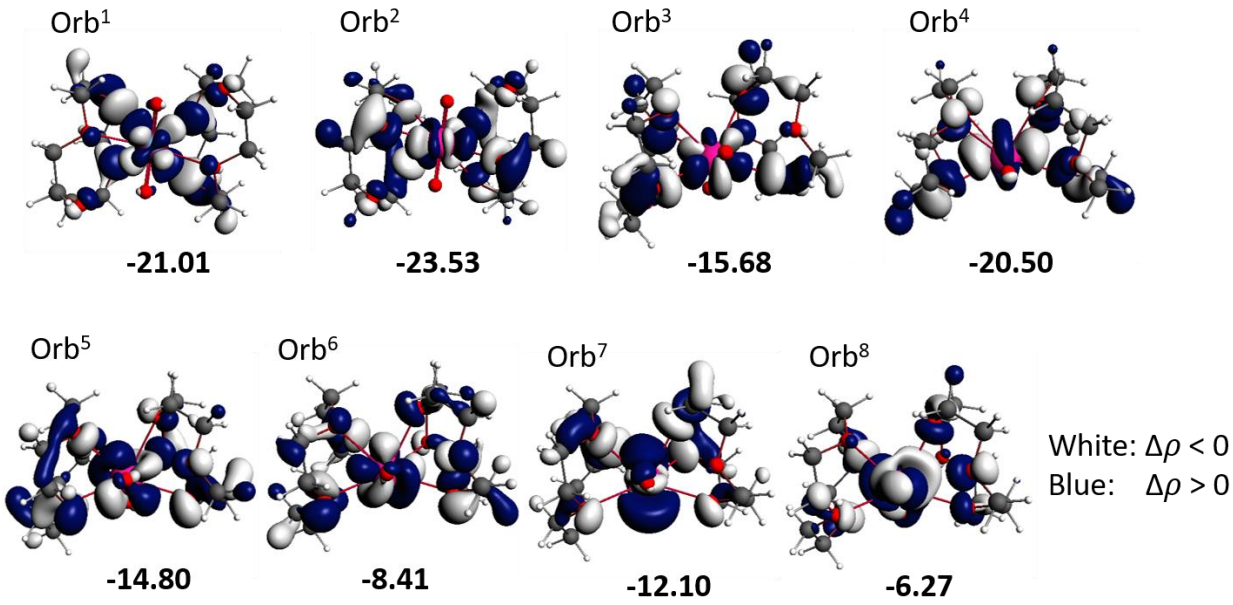

Figure 7. Plot of representative U-O bonding interaction between UO_2^{2+} and 12C4 ligand fragments from ETS-NOCV method with a closed-shell PBE calculation (energy units = kcal/mol, isovalue =0.03).

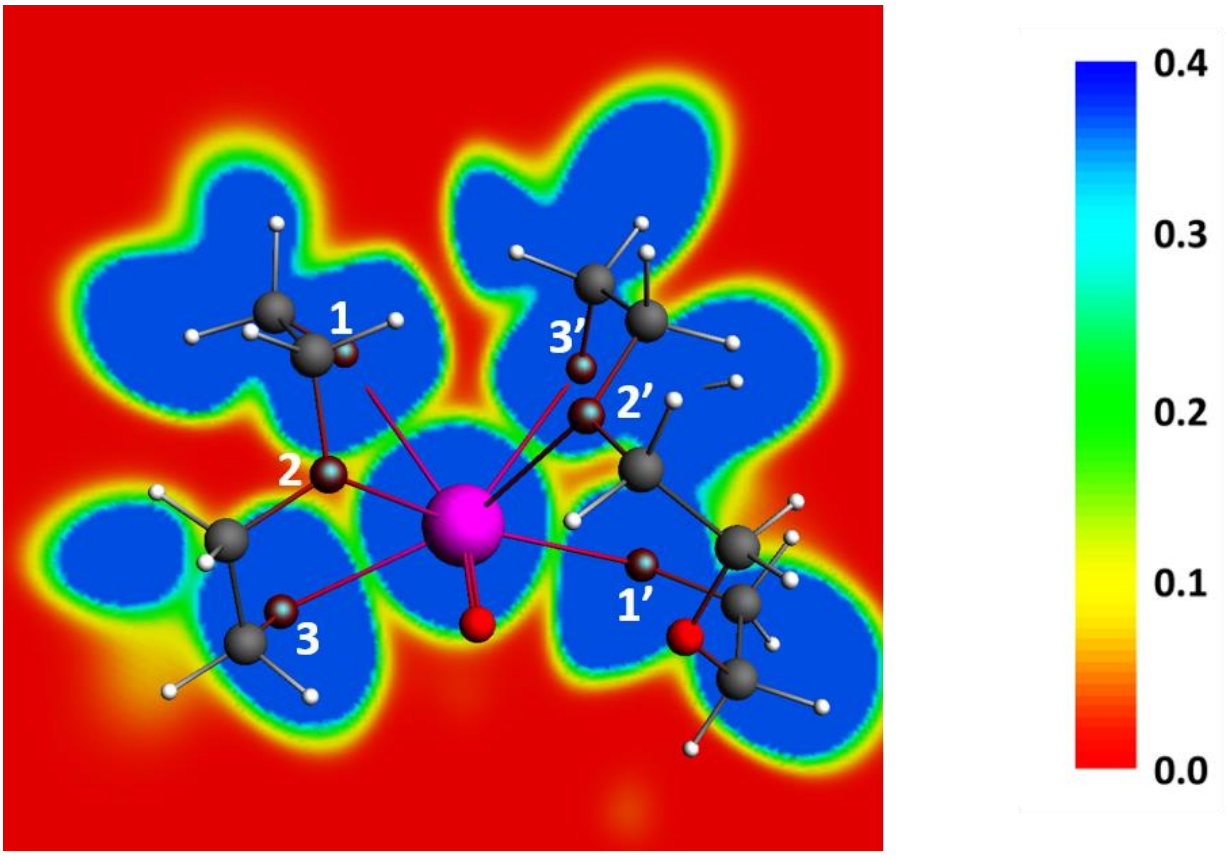

Figure 8. Two-dimensional ELF contour for the O-U-O planes containing the U-O interaction. The results are based on the SR-ZORA-PBE calculated densities.

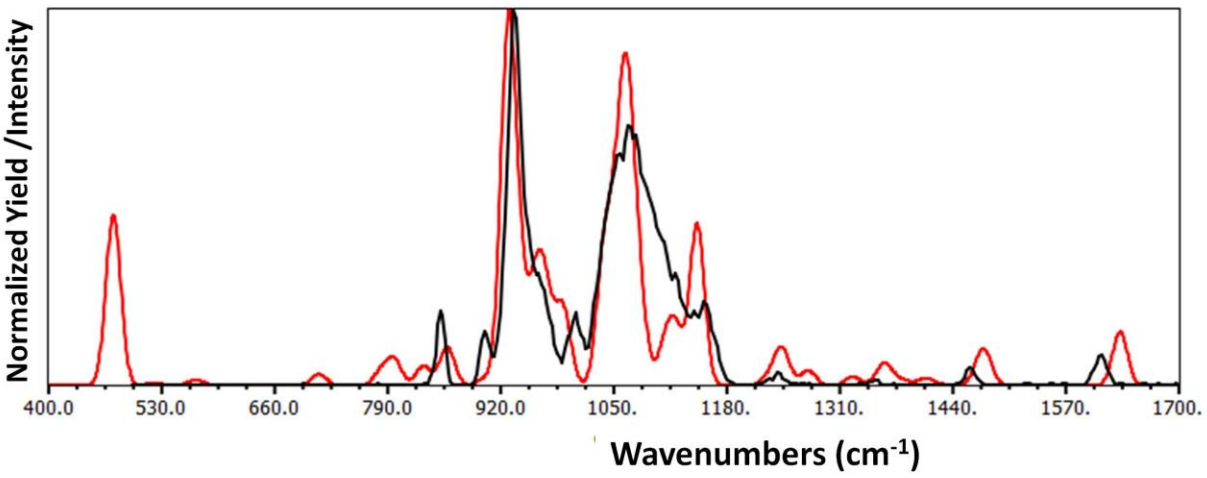

Figure 9. IRMPD spectrum of $[UO_2(12C4\text{-}H)]^+$ is in black. In red is the computed IR spectrum for the GS structure.

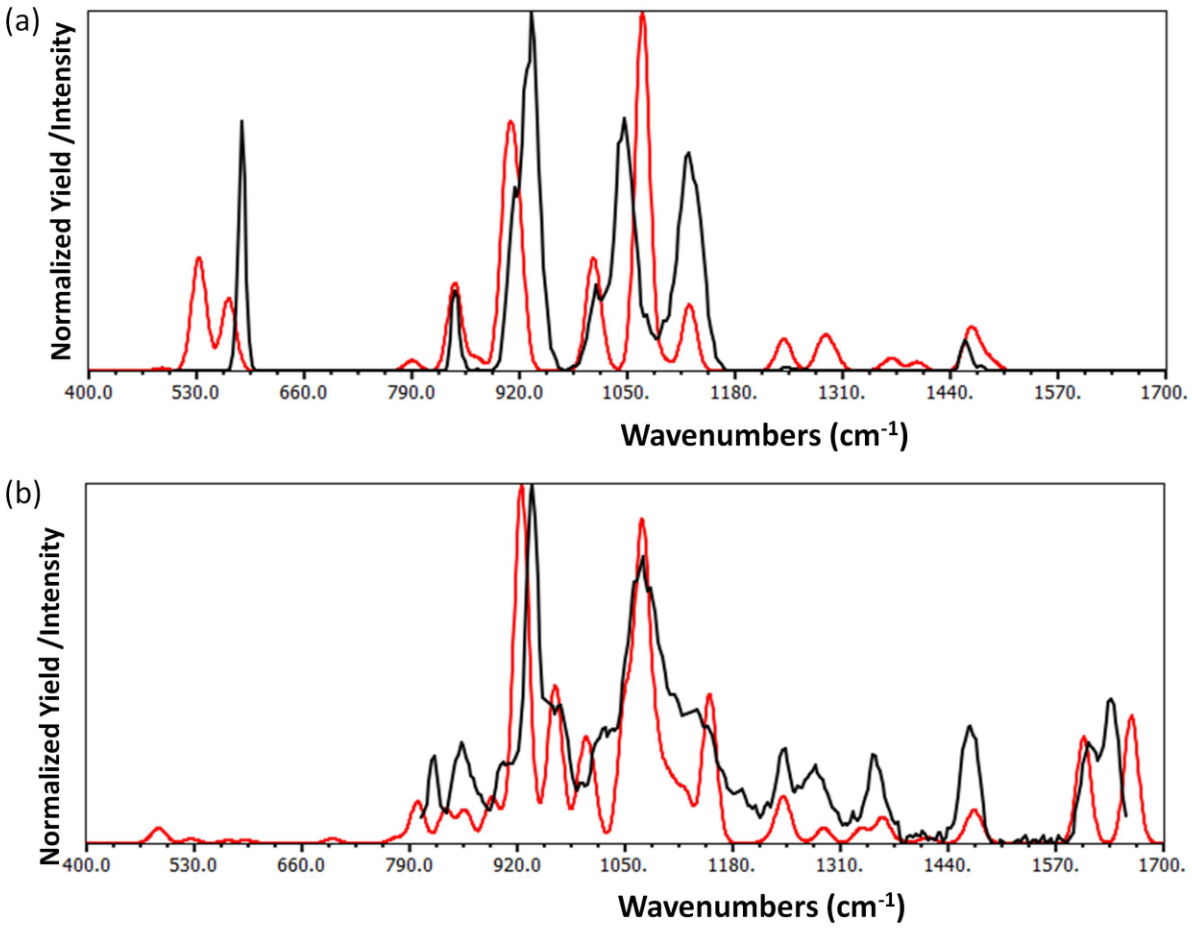

Figure 10. IRMPD spectra of (a) $[UO_2(12C4)(OH)]^+$ from reaction (2), and (b) $[UO_2(12C4\text{-}H)(H_2O)]^+$ from reaction (3) are in black. In red are the computed spectra for the GS structures.

Table of Contents

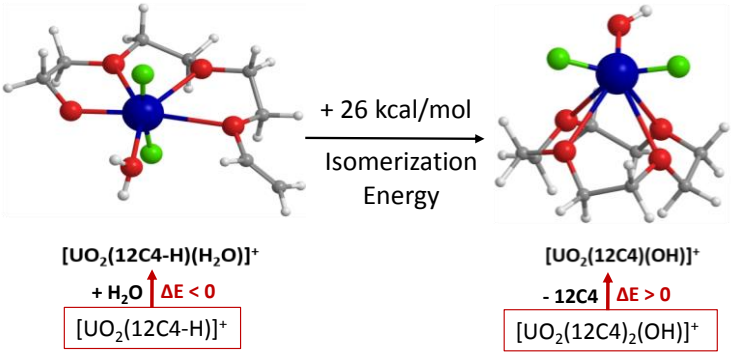

Distinctive structures of gas-phase uranyl/12-Crown-4 coordination complexes include a species in which a C-O bond has been cleaved. Relatively high ether coordination is achieved absent competition with more strongly coordinating ligands as occurs in condensed phase. Two isomers were alternatively produced by exothermic hydration and endothermic ligand elimination.